# Critical behaviour in the QCD Anderson transition

Matteo Giordano, Tamás G. Kovács and Ferenc Pittler

Institute for Nuclear Research (ATOMKI), Debrecen

Lattice 2013
Mainz, 31st July 2013

# Spectrum of the Dirac Operator

Dirac operator (in Euclidean space) $\not{D}$

- anti-Hermitian: purely imaginary spectrum
- $\{\not{D}, \gamma_5\} = 0$: symmetric w.r.t $\lambda = 0$

Chiral condensate in the chiral limit ⇔ spectral density at the origin
[Banks, Casher (1980)]

$$\langle\bar{\psi}\psi\rangle = \lim_{m\to 0}\lim_{V\to\infty}\frac{\pi\rho(0)}{V} \qquad \rho(\lambda) = \left\langle \sum_i \delta(\lambda - \lambda_i)\right\rangle$$

Different localisation properties of the low-lying eigenmodes below and above the chiral-crossover temperature $T_c$

- $T < T_c$: extended
- $T > T_c$: localised

# Localisation in the Dirac Spectrum

Low-lying modes are localised above the chiral-crossover temperature $T_c$
[Garcia-Garcia, Osborn (2007), Kovács (2010), Kovács, Pittler (2010), Kovács, Pittler (2012)]

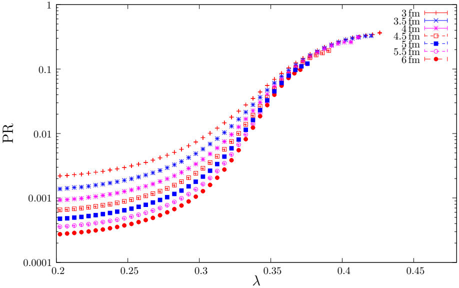


$$\mathrm{IPR} = \sum_x |\psi(x)|^4$$

$$\mathrm{PR} = \mathrm{IPR}^{-1}/V_4$$

$NT = 4,\ \beta = 3.75$

$\ell = a \cdot \mathrm{IPR}^{-1/4} \sim$ loc. length

$\ell_{\mathrm{localised}} \sim T^{-1}$

- Eigenmodes localised for $\lambda < \lambda_c(T)$
- No localised modes in the chirally broken phase: $\lambda_c(T_c) \sim 0$
- $\lambda_c \sim$ effective gap: low-lying modes do not contribute to hadronic correlators at large distance

# Anderson Model in 3D

Tight-binding Hamiltonian for "dirty" conductors

$$H = \sum_n \varepsilon_n |n\rangle\langle n| + \sum_{n,\mu} |n+\hat{\mu}\rangle\langle n| + |n\rangle\langle n+\hat{\mu}|$$

$\varepsilon_n$: random on-site potential (width $W \sim$ disorder), $|n\rangle$: localised states

- No disorder ($W = 0$): delocalised eigenstates
- Nonzero disorder: eigenstates at the band edge become localised due to destructive interference (Anderson localisation) [Anderson (1958)]

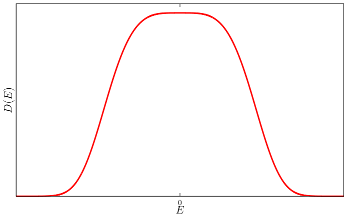


As $W$ increases, $E_c$ moves towards the band center, for $W > W_c$ all the states become localised: metal-insulator transition

# Anderson Model in 3D

Tight-binding Hamiltonian for "dirty" conductors

$$H = \sum_n \varepsilon_n |n\rangle\langle n| + \sum_{n,\mu} |n+\hat{\mu}\rangle\langle n| + |n\rangle\langle n+\hat{\mu}|$$

$\varepsilon_n$: random on-site potential (width $W \sim$ disorder), $|n\rangle$: localised states

- No disorder ($W = 0$): delocalised eigenstates
- Nonzero disorder: eigenstates at the band edge become localised due to destructive interference (Anderson localisation) [Anderson (1958)]

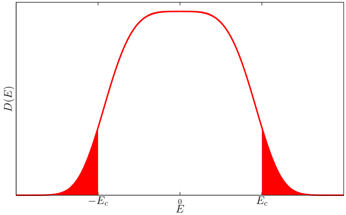


As $W$ increases, $E_c$ moves towards the band center, for $W > W_c$ all the states become localised: metal-insulator transition

# Anderson Model in 3D

Tight-binding Hamiltonian for "dirty" conductors

$$H = \sum_n \varepsilon_n |n\rangle\langle n| + \sum_{n,\mu} |n+\hat{\mu}\rangle\langle n| + |n\rangle\langle n+\hat{\mu}|$$

$\varepsilon_n$: random on-site potential (width $W \sim$ disorder), $|n\rangle$: localised states

- No disorder ($W = 0$): delocalised eigenstates
- Nonzero disorder: eigenstates at the band edge become localised due to destructive interference (Anderson localisation) [Anderson (1958)]

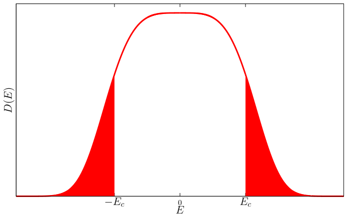


As $W$ increases, $E_c$ moves towards the band center, for $W > W_c$ all the states become localised: metal-insulator transition

# Anderson Model in 3D

Tight-binding Hamiltonian for “dirty” conductors

$$H = \sum_n \varepsilon_n |n\rangle\langle n| + \sum_{n,\mu} |n+\hat{\mu}\rangle\langle n| + |n\rangle\langle n+\hat{\mu}|$$

$\varepsilon_n$: random on-site potential (width $W \sim$ disorder), $|n\rangle$: localised states

- No disorder ($W = 0$): delocalised eigenstates
- Nonzero disorder: eigenstates at the band edge become localised due to destructive interference (Anderson localisation) [Anderson (1958)]

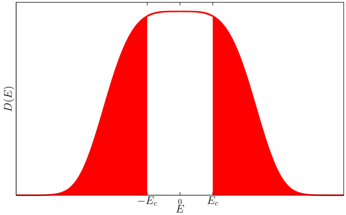


As $W$ increases, $E_c$ moves towards the band center, for $W > W_c$ all the states become localised: metal-insulator transition

# Anderson Model in 3D

Tight-binding Hamiltonian for "dirty" conductors

$$H = \sum_n \varepsilon_n |n\rangle\langle n| + \sum_{n,\mu} |n+\hat{\mu}\rangle\langle n| + |n\rangle\langle n+\hat{\mu}|$$

$\varepsilon_n$: random on-site potential (width $W \sim$ disorder), $|n\rangle$: localised states

- No disorder ($W = 0$): delocalised eigenstates
- Nonzero disorder: eigenstates at the band edge become localised due to destructive interference (Anderson localisation)
  [Anderson (1958)]

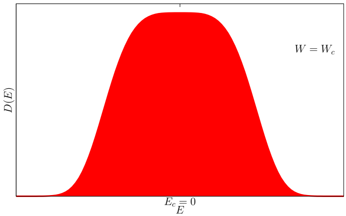


As $W$ increases, $E_c$ moves towards the band center, for $W > W_c$ all the states become localised: metal-insulator transition

# Analogies and Differences Between AM and QCD

Anderson Model

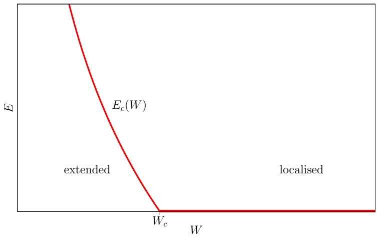


QCD

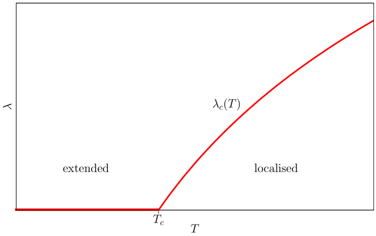


Localised modes $\leftrightarrow$ low spectral density
Modes not mixed by fluctuations $\rightarrow$ Poisson statistics

Extended modes $\leftrightarrow$ high spectral density
Modes mixed by fluctuations $\rightarrow$ Random Matrix Theory statistics

Most conveniently checked using the unfolded spectrum
Unfolding: local rescaling of eigenvalues $\lambda_i \rightarrow \frac{\lambda_i}{\langle \lambda_{i+1} - \lambda_i \rangle}$

# Spectrum of the Dirac Operator above $T_c$

Symanzik improved gauge action, 2+1 stout smeared staggered fermions
[Budapest-Wuppertal collaboration]

$N_T = 4$, $\beta = 3.75 \to T = 394\,\mathrm{MeV} = 2.6\,T_c$, $a = 0.125\,\mathrm{fm}$

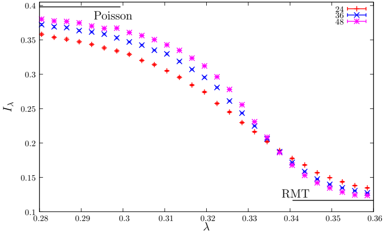


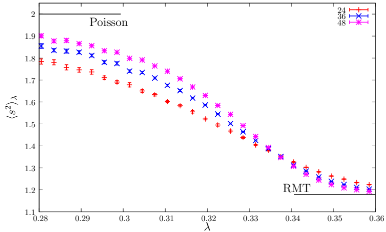


$$I_\lambda = \int_0^{s_0} ds\, P_\lambda(s)\,, \quad s_0 \simeq 0.5 \qquad \langle s^2\rangle_\lambda = \int_0^\infty ds\, P_\lambda(s)\, s^2$$

$$s = \frac{\lambda_{i+1}-\lambda_i}{\langle\lambda_{i+1}-\lambda_i\rangle}$$

Curve becomes steeper as the volume is increased $\to$ true phase transition

# Anderson Transition

3D Anderson model: metal-insulator second-order phase transition
Divergent correlation length at critical disorder $W_c$/at mobility edge $E_c$:

$$\xi_\infty(W) \propto |W - W_c|^{-\nu} \qquad \xi_\infty(E) \propto |E - E_c|^{-\nu}$$

Finite volume $L^3$, take $Q(E, L)$ such that
[Shklovskii et al. (1993), Hofstatter and Schreiber (1994), Siringo, Piccitto (1998)]

$$\lim_{L\to\infty} Q(E, L) = \begin{cases} Q_m & E < E_c \quad \text{(metallic side)} \\ Q_c & E = E_c \quad \text{(critical point)} \\ Q_i & E > E_c \quad \text{(insulator side)} \end{cases}$$

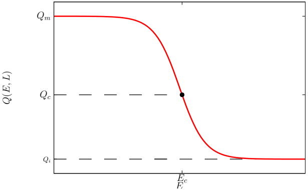


Finite-size scaling: $Q(E, L) = f(L/\xi_\infty(E)) = F(L^{1/\nu}(E - E_c))$

$$Q(E, L) \simeq Q(E_c, L) + Q'(E_c, L)(E - E_c) = F(0) + F'(0)L^{1/\nu}(E - E_c)$$

# Anderson Transition in the Dirac Spectrum

Use one-parameter scaling to all orders to measure $\nu$ and $\lambda_c$

$$Q(\lambda, L) = f(L/\xi_\infty(\lambda)) = F(L^{1/\nu}(\lambda - \lambda_c)) = \sum_{n=0}^{\infty} \frac{F^{(n)}(0)}{n!} L^{n/\nu}(\lambda - \lambda_c)^n$$

- Use several volumes in a two-variable fit
- Estimate the systematic error through constrained (Bayesian) fits including more and more terms in the expansion

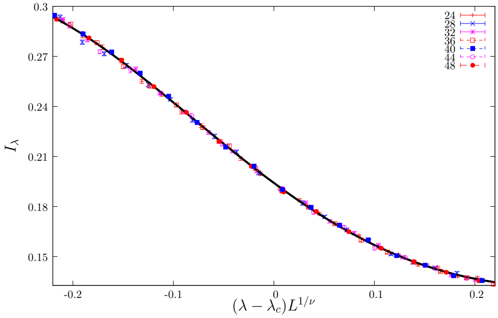


$Q = I_\lambda = \int_0^{s_0} ds\, P_\lambda(s)$

# Critical Exponent

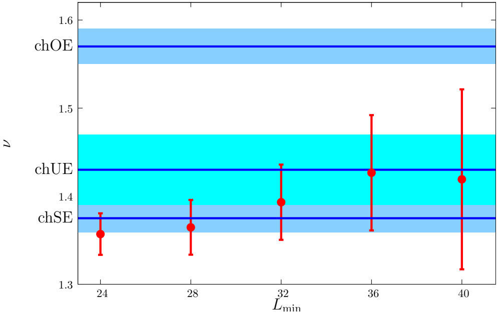


## Anderson model 3D

$$\nu_{\rm chSE} = 1.375 \pm 0.016$$
$$\nu_{\rm chUE} = 1.43 \pm 0.04$$
$$\nu_{\rm chOE} = 1.57 \pm 0.02$$

[Slevin, Ohtsuki (1997), (1999), Asada *et al.*, (2005)]

## QCD

$$\nu = 1.425(65)$$
$$(L_{\rm min} = 36)$$

details

# Critical Exponent

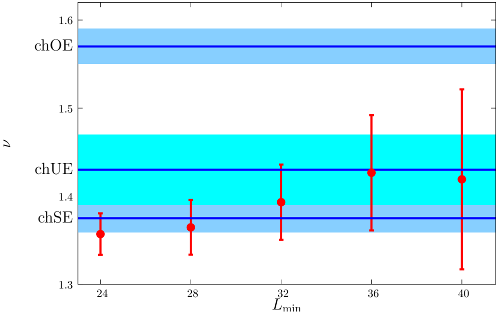


**Anderson model 3D**

$$\nu_{\text{chSE}} = 1.375 \pm 0.016$$
$$\nu_{\text{chUE}} = 1.43 \pm 0.04$$
$$\nu_{\text{chOE}} = 1.57 \pm 0.02$$

[Slevin, Ohtsuki (1997), (1999), Asada *et al.*, (2005)]

**QCD**

$$\nu = 1.425(65)$$
$$(L_{\min} = 36)$$

details

# Shape Analysis

Plot two observables against each other, if points collapse on a single curve $\rightarrow$ universal path in the space of probability distribution [Varga et al. (1995)]

Family of RM models connecting Poisson $\leftrightarrow$ RMT [talk by S.M. Nishigaki]

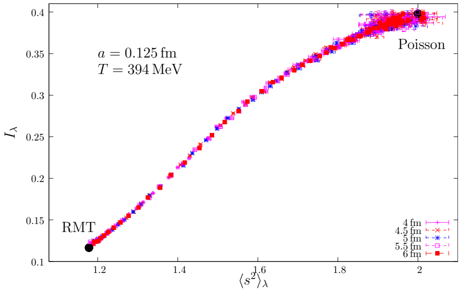


Points flow towards the Poisson and RMT “fixed points” as $L \rightarrow \infty$

Unstable fixed point $\approx$ critical point, different universality class

Universal path also changing $T$ or $a$?

# Shape Analysis

Plot two observables against each other, if points collapse on a single curve
$\rightarrow$ universal path in the space of probability distribution [Varga et al. (1995)]

Family of RM models connecting Poisson $\leftrightarrow$ RMT [talk by S.M. Nishigaki]

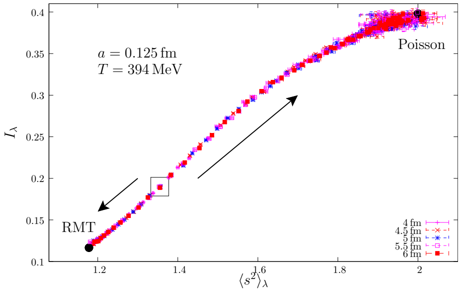


Points flow towards the Poisson and RMT "fixed points" as $L \rightarrow \infty$

Unstable fixed point $\approx$ critical point, different universality class

Universal path also changing $T$ or $a$?

# Shape Analysis

Plot two observables against each other, if points collapse on a single curve $\rightarrow$ universal path in the space of probability distribution [Varga et al. (1995)]

Family of RM models connecting Poisson $\leftrightarrow$ RMT [talk by S.M. Nishigaki]

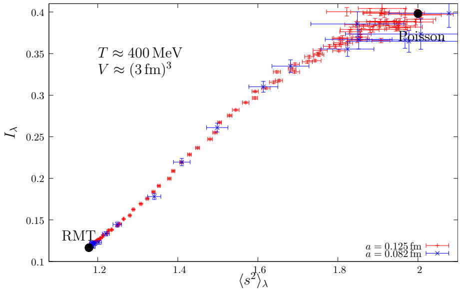


Points flow towards the Poisson and RMT "fixed points" as $L \rightarrow \infty$

Unstable fixed point $\approx$ critical point, different universality class

Universal path also changing $T$ or $a$?

# Shape Analysis

Plot two observables against each other, if points collapse on a single curve $\rightarrow$ universal path in the space of probability distribution [Varga et al. (1995)]

Family of RM models connecting Poisson $\leftrightarrow$ RMT [talk by S.M. Nishigaki]

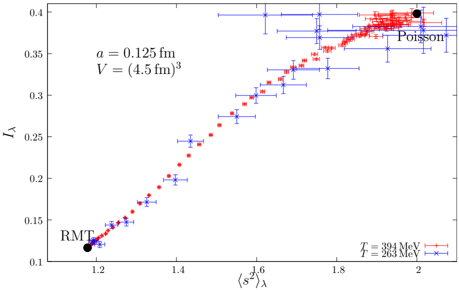


Points flow towards the Poisson and RMT "fixed points" as $L \rightarrow \infty$

Unstable fixed point $\approx$ critical point, different universality class

Universal path also changing $T$ or $a$?

# Summary and Outlook

- Dirac spectrum above $T_c$ shows a localisation/delocalisation transition analogous to the Anderson transition in condensed matter
- Critical exponent consistent with Anderson model: same universality class?

Open issues:

- Inclusion of corrections to scaling
- Study of the multifractal structure of eigenmodes near the transition

# References


- T. Banks and A. Casher, *Nucl. Phys. B* **169** (1980) 103
- A.M. Garcia-Garcia and J.C. Osborn, *Phys. Rev. D* **75** (2007) 034503
- T.G. Kovács, *Phys. Rev. Lett.* **104** (2010) 031601
- T.G. Kovács and F. Pittler, *Phys. Rev. Lett.* **105** (2010) 192001
- T.G. Kovács and F. Pittler, *Phys. Rev. D* **86** (2012) 114515
- P.W. Anderson, *Phys. Rev.* **109** (1958) 1492
- I. Varga, E. Hofstatter, M. Schreiber and J. Pipek, *Phys. Rev. B* **52** (1995) 7783
- E. Hofstatter and M. Schreiber, *Phys. Rev. B* **49** (1994) 14726
- B.I. Shklovskii, B. Shapiro, B.R. Sears, P. Lambrianides and H.B. Shore, *Phys. Rev. B* **47** (1993) 11487
- F. Siringo and G. Piccitto, *J. Phys. A* **31** (1998) 5981
- K. Slevin and T. Ohtsuki, *Phys. Rev. Lett.* **78** (1997) 4083; *Phys. Rev. Lett.* **82** (1999) 382; Y. Asada, K. Slevin and T. Ohtsuki, *J. Phys. Soc. Jpn.* **74** supplement (2005) 258

# Critical Exponent: Details

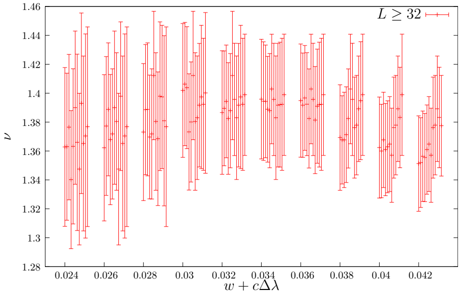


Check possible systematic effects due to the choice of the fitting range and of the width of the bins

$$I_\lambda \to \int_{B_{\Delta\lambda}(\lambda)} d\lambda' \, I_{\lambda'} \rho(\lambda') \Big/ \int_{B_{\Delta\lambda}(\lambda)} d\lambda' \, \rho(\lambda')$$

back

# Critical Exponent: Details

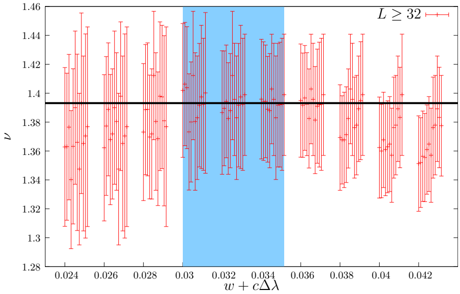


Check possible systematic effects due to the choice of the fitting range and of the width of the bins

$$I_\lambda \to \int_{B_{\Delta\lambda}(\lambda)} d\lambda' \, I_{\lambda'} \rho(\lambda') \Big/ \int_{B_{\Delta\lambda}(\lambda)} d\lambda' \, \rho(\lambda')$$

back